

Vivianite recovery from anaerobic groundwater reverse osmosis concentrate

Goedhart, Roos; Koudijs, Nienke; van Loosdrecht, Mark C.M.; van Halem, Doris

10.1016/j.watres.2025.124101

Publication date

Document Version Final published version

Published in Water Research

Citation (APA)

Goedhart, R., Koudijs, N., van Loosdrecht, M. C. M., & van Halem, D. (2025). Vivianite recovery from anaerobic groundwater reverse osmosis concentrate. Water Research, 285, Article 124101. https://doi.org/10.1016/j.watres.2025.124101

Important note

To cite this publication, please use the final published version (if applicable). Please check the document version above.

Other than for strictly personal use, it is not permitted to download, forward or distribute the text or part of it, without the consent of the author(s) and/or copyright holder(s), unless the work is under an open content license such as Creative Commons.

Takedown policy

Please contact us and provide details if you believe this document breaches copyrights. We will remove access to the work immediately and investigate your claim.

ELSEVIER

Contents lists available at ScienceDirect

Water Research

journal homepage: www.elsevier.com/locate/watres



Vivianite recovery from anaerobic groundwater reverse osmosis concentrate

Roos Goedhart ^{a,*} , Nienke Koudijs ^b, Mark C.M. van Loosdrecht ^c, Doris van Halem ^a

- a Water Management Department, Faculty of Civil Engineering and Geosciences, Delft University of Technology, Stevinweg 1, 2628 CN, Delft, the Netherlands
- ^b Brabant Water N.V., Minervum 7181, 4817 ZN Breda, the Netherlands
- ^c Biotechnology Department, Faculty of Applied Sciences, Delft University of Technology, Van der Maasweg 9, Delft 2629 HZ, the Netherlands

ARTICLE INFO

Keywords: Groundwater Membrane filtration RO concentrate Treatment Iron Vivianite

ABSTRACT

To meet the increasing drinking water demand, membrane technologies are used to treat previously unavailable water sources. A byproduct of membrane technologies is the concentrate stream, containing valuable resources in higher concentrations. We studied the recovery of iron from different groundwater matrices and anaerobic reverse osmosis (RO) concentrates via precipitation of vivianite and the co-removal of other common groundwater divalent cations Mn^{2+} , Mg^{2+} and Ca^{2+} during vivianite precipitation. The formed precipitates were characterized using X-Ray Diffraction and Scanning Electron Microscopy. Vivianite precipitation removed a maximum of 89 % of Fe^{2+} in raw groundwater and 52 % Fe^{2+} from RO concentrate. Substantial co-removal of Mn^{2+} (max 91 %) and limited co-removal of Mg^{2+} (max 7 %) were found, without hindering Fe removal efficiencies or altering morphological changes of the vivianite crystal. In contrast, co-removal of Ca^{2+} occurred at the expense of iron removal, forming amorphous calcium phosphate precipitates. This study shows the potential of vivianite precipitation for iron recovery across a wide range of groundwater matrices and highlights the need for further research to optimize this novel method to treat concentrate streams that are challenging to dispose of.

1. Introduction

Groundwater in deep anaerobic aquifers is recognized for its excellent quality, making it a popular source for drinking water. A natural and common contaminant in anaerobic groundwater is iron (Fe²⁺). Drinking water can contain a maximum concentration of 0.3 mg Fe/L (World Health Organization, 2017). Membrane technologies, such as reverse osmosis (RO), are highly effective in removing iron, alongside other contaminants that are increasingly found in groundwater sources due to increasing pressure of human activities (e.g., pesticides (Schipper et al., 2008)) and climate variability (e.g., salinization (Zamrsky et al., 2024)). However, membrane technologies produce a byproduct stream called 'concentrate'. Currently, the concentrate is often discharged on surface waters or in wastewater treatment plants. With the increasing use of membrane technologies, it is expected that legislation around concentrate disposal will become stricter (Nederlof et al., 2005). Additionally, the concentrate stream contains valuable resources (Pérez-González et al., 2012).

Another common and more ancient treatment method for iron removal from groundwater is aeration followed by sand filtration. In this

process, Fe²⁺ is oxidized to Fe³⁺, which precipitates immediately as iron flocs (Fe(OH)₃) (Van Beek et al., 2012). The flocs are subsequently retained in the filter bed and thereby removed from the water stream (Müller et al., 2024). Removal of iron comes with several challenges. The formed flocs clog the filter bed, requiring frequent backwashing (Haukelidsaeter et al., 2024). The water needed for backwashing and the temporary interruption of the treatment process decreases the overall efficiency of the plant, making it a cost-intensive step (Turner et al., 2019). Moreover, backwashing generates a substantial byproduct stream of iron sludge. In The Netherlands alone, this stream accounts for \pm 100,000 ton/year (AquaMinerals, 2020).

As an alternative to oxidation and filtration, Fe^{2+} can be recovered from anaerobic water via vivianite ($Fe_3(PO_4)_2$) precipitation (Goedhart et al., 2022). This novel process in the industry could lead to the valorisation of iron sludge as a byproduct. The sludge volume can be reduced to a third, while the halftime for iron removal during vivianite precipitation was four times lower compared to iron oxidation and filtration. This approach can contribute to the design of more efficient filters, which results in fewer interruptions and water losses.

For groundwater-relevant iron concentrations (<25 mg/L), the

E-mail address: r.c.goedhart@tudelft.nl (R. Goedhart).

 $^{^{\}ast}$ Corresponding author.

R. Goedhart et al. Water Research 285 (2025) 124101

saturation index (SI) for vivianite requires a relatively high pH (Goedhart et al., 2022). Alternatively, elevating the iron concentrations prior to vivianite precipitation also increases the SI. Therefore, vivianite precipitation to recover iron from anaerobic RO concentrate is tested in this study, contributing to the growing implementation of resource recovery strategies in water treatment.

The concentrate will also contain elevated levels of other cations. It is known that the ${\rm Fe}^{2+}$ in the vivianite crystal can be substituted by several other divalent cations (Kloprogge et al., 2003; Rothe et al., 2016). Especially ${\rm Mn}^{2+}$ and ${\rm Mg}^{2+}$ are frequently present in the vivianite lattice in natural environments (Kubeneck et al., 2023; Rothe et al., 2016) and ${\rm Ca}^{2+}$ can compete with ${\rm Fe}^{2+}$ for phosphate and inhibit vivianite growth by covering its surface (Cao et al., 2023). The divalent cations ${\rm Mn}^{2+}$, ${\rm Mg}^{2+}$ and ${\rm Ca}^{2+}$ are common groundwater constituents. This study therefore also examines how ${\rm Mn}^{2+}$, ${\rm Mg}^{2+}$ and ${\rm Ca}^{2+}$ are removed from groundwater alongside ${\rm Fe}^{2+}$ during vivianite precipitation. To do so, ${\rm Fe}^{2+}$ removal via vivianite precipitation was tested in different water matrices containing groundwater and concentrate relevant concentrations of ${\rm Mn}^{2+}$, ${\rm Mg}^{2+}$ and ${\rm Ca}^{2+}$. The formed precipitates were analyzed by X-Ray Diffraction (XRD) and visualized by Scanning Electron Microscopy (SEM).

2. Materials & methods

2.1. Groundwater and concentrate composition

Vivianite precipitation was tested in different water matrices and under different conditions. The composition of these different water matrices is given in Table 1. Experiments on site were performed at two different drinking water treatment plants of drinking water company Vitens (Netherlands): locations Witharen and Spannenburg. From now on we refer to these sites as TP1 and TP2. Experiments were performed using both natural groundwater and untreated concentrate streams, produced by the anaerobic RO units. At TP1 the natural $\rm Fe^{2+}$ concentration was 8.4 mg/L and the pH 6.8; at TP2 Fe was present at 12.8 mg/L and the pH was 6.9.

At the third water treatment plant (Hammerflier), referred to as TP3 from now on, the natural concentration of Fe^{2+} in groundwater was the highest: 24.7 mg/L. The pH of the raw groundwater of TP3 was 7.1. This treatment plant does not have an RO step and therefore iron removal was solely tested in groundwater. The experiments with groundwater of TP3 were not performed on-site, but the water was transported to the lab and experiments were conducted in an anaerobic environment. The same was done with all experiments with groundwater obtained from Loosdrecht (TP4); this treatment plant does not have an RO step either. With this water the individual effect of divalent ions Mn^{2+} , Mg^{2+} and Ca^{2+} on vivianite precipitation was tested by dosing desired

Table 1 Composition of the raw groundwater of treatment plant (TP) 1 (Witharen), TP2 (Spannenburg), TP3 (Hammerflier) and TP4 (Loosdrecht) and composition of the RO concentrate (conc) streams (only applicable to TP1 and TP2). EC = Electrical Conductivity.

		TP1		TP2		TP3	TP4
		Raw	Conc	Raw	Conc	Raw	Raw
Fe	mg/l	12.8	62.6	8.4	41.4	24.7	4.3
Mn	mg/l	0.5	2.4	0.3	1.6	0.3	0.2
Ca	mg/l	124	609	93	461	73	38.5
Mg	mg/l	10.5	48.0	6.5	30.0	4.3	2.2
EC	mS/m	68.5	214	53.0	182	41.1	23.3
pН	pН	6.9	7.3	6.8	7.3	7.1	7.3
HCO_3	mg/l	437	2130	335	1556	247	120
NH_4	mg/l	3.3	14.8	1.3	6.0	2.84	0.3
NO_3	mg/l	1.7	3.7	< 0.2	<1.0	< 0.2	< 0.2
Na	mg/l	18.3	73.0	22.9	106	14.4	9.0
Cl	mg/l	36	171	31	143	23	15

concentrations of the required ions. This groundwater was chosen because it has relatively low concentrations of divalent cations, and previous experiments in Goedhart et al. (2022) have demonstrated that vivianite can indeed precipitate in this matrix. The water obtained from TP4 was taken and handled in accordance with the description in Goedhart et al. (2022).

2.2. On-site anaerobic groundwater and RO concentrate experiments

The recovery of Fe²⁺ through vivianite precipitation was studied in batch experiments at TP1 and TP2. Both anaerobic groundwater and anaerobic concentrate were used in these experiments. A bottle was filled from the bottom and overflown for 3 min before closing it with an airtight rubber cap, to maintain anaerobic conditions in the bottle. A closed, empty syringe was introduced as pressure release, such that the base and phosphate solutions could be added to the completely full bottles. The bottles were placed on a magnetic mixer plate. A picture of the setup is given in Figure S1. The pH was adjusted by dosing anaerobically prepared 0.1 M NaOH (Sigma Aldrich). Afterwards, phosphate was slightly overdosed in a 1:1 molar ratio to Fe²⁺, using an anaerobically prepared 0.1 M Na₃PO₄ solution (Sigma Aldrich) of pH 8. Two samples of 5 mL were taken during the experiment: directly after base dosing, and 30 min after phosphate dosing. The samples were immediately filtered over a 0.2 µm filter and acidified to 1-2 % v/v HNO₃ (Carl Roth ROTIPURAN®Supra 69 %). The pH was measured at the end of the experiment, by opening the bottle and using a HACH Sension+ MM150 portable multimeter.

2.3. Anaerobic groundwater experiments in the laboratory

Water from TP3 and TP4 was transported anaerobically to the laboratory, in which experiments were performed in an anaerobic chamber (Coy Laboratory Products, USA), containing a gas mixture of 5 % hydrogen and 95 % argon gas (impurity <200 vpm). The chamber had an airlock and weekly regenerated palladium catalysts to secure anaerobic conditions. Anaerobic conditions were monitored using an oxygen analyzer (CAM-10, Coy Lab). Water vapor was entrapped by silica beads to keep the humidity below 70 %. The experiments using the water from TP3 were similar as described in 2.2, but then performed in the anaerobic chamber instead of in the field, obviating the need for the airtight rubber cap.

The interaction of divalent ions Mn²⁺, Mg²⁺ and Ca²⁺ on vivianite precipitation was studied with water from TP4. Filtered anaerobic groundwater of TP4 was spiked with 2.5 mL of 0.179 M FeCl₂·4 H₂O (Sigma Aldrich), which makes the total Fe²⁺ concentration the sum of the spiked 1.79 mM (100 mg Fe/L), and the naturally present 0.077 mM of Fe²⁺ (see Table 1). This equals 104.3 mg/L. Additionally, the water was spiked with either Mn²⁺ (MnCl₂·4H₂O), Mg²⁺ (MgCl₂·6H₂O) or Ca²⁺ (CaCl₂·2H₂O) to obtain concentrations as listed in Table 2. The concentrations spiked were chosen based on the concentrations present in natural groundwater and RO concentrate streams. Note that the background concentrations of Mg²⁺, Mn²⁺ and Ca²⁺ in water from TP4

Table 2 Concentrations of Ca^{2+} , Mg^{2+} and Mn^{2+} dosed in the different experiments. Only one of these three compounds was dosed in each experiment.

	Ca ²⁺		Mg ²⁺		Mn ²⁺	
	mg/l	mM	mg/l	mM	mg/l	mM
I	0	0	10	0.4	0.5	0.009
II	100	2.5	40	1.6	2	0.04
III	200	5	80	3.3	5	0.09
IV	400	10				
V	600	15				
VI	800	20				
VII	1000	25				

are 2.2, 0.2 and 38.5 mg/L respectively (Table 1). The reactions were initialized by spiking the jar with 4.5 mL 0.1 M $\rm Na_3PO_4$ to obtain a 1:1 molar ratio of Fe:PO_4. Samples of 10 mL were taken just before, and 15 min after phosphate dosing. The samples were immediately filtered over a 0.2 μm nanopore filter and acidified using 1 % v/v 65 % HNO_3 upon removal from the anaerobic chamber. The pH was measured using the HACH Sension+ MM150 multimeter. After the experiment, the water was vacuum filtered over hydrophilic membrane filters (0.15–0.22 μm). These filters were covered in aluminum foil and stored in the anaerobic chamber until analysis.

2.4. Analysis

The concentrations of divalent ions and phosphorus in the water samples were measured using ICP-OES (Optima 8000, PerkinElmer). The samples were diluted beforehand in 3 % HNO $_3$ to obtain concentrations in the range of 0.1 – 10 mg/L. A paired t-test was conducted to evaluate whether the removal percentage of the divalent cations significantly increased after adding either NaOH or Na $_3$ PO $_4$. Unless mentioned otherwise, the results presented are statistically significant (p < 0.05)

The precipitates formed were characterized by X-ray diffraction (XRD), using a Bruker D8 Advance with $CuK\alpha1$ radiation (40 kV, 25 mA). A reference pattern from Morris et al. was used to verify the presence of vivianite in different samples (Morris et al., 1979). From each experiment of TP4, at least one of the precipitates was analyzed by scanning electron microscopy (SEM) (Novanano, FEI, Thermo Fischer) equipped with EDAX electron dispersive X-ray spectrometer (EDX) for chemical elements investigation at an acceleration voltage of 7.00 kV.

3. Results

3.1. Co removal of divalent ions during vivianite precipitation in anaerobic groundwater

Vivianite precipitation to remove Fe^{2+} was investigated in different groundwater matrices. Fig. 1 shows the Fe^{2+} removal and co-removal of divalent ions Mg^{2+} , Mn^{2+} and Ca^{2+} after addition of a base and phosphate at TP1, TP2 and TP3. Phosphate addition to anaerobic groundwater removed Fe^{2+} in all water matrices. The highest removal efficiency found was at TP3, with 89 % Fe^{2+} removal at pH 9. The initial Fe^{2+} concentration at TP3 was 2–3 times higher compared to TP2 and TP1. An increase in pH enhanced Fe^{2+} removal, consistent with previous findings (Goedhart et al., 2022). The experiments using TP3 water were performed in an anaerobic chamber, preventing oxidation of the formed solids. These solids were analyzed by XRD: at pH 7 and 8 only vivianite was detected, but an amorphous structure was found at pH 9 (Figure S2). Fig. 1a shows that at pH 9, the addition of the base NaOH already resulted in Fe^{2+} removal up to 53 %, which likely precipitated into amorphous structures as detected by XRD.

The removal efficiencies of $\rm Mn^{2+}$ were similar to $\rm Fe^{2+}$, showing a maximum removal of 87 % at pH 9 at TP3 (Fig. 1b). The $\rm Mn^{2+}$ concentrations in the groundwater were, however, 100 times lower compared to $\rm Fe^{2+}$ (Table 1). $\rm Ca^{2+}$ was present in higher concentrations and a maximum removal efficiency of 30 % was found at pH 9, corresponding to 23 mg/L removed (Fig. 1c). No significant removal of $\rm Mg^{2+}$ by phosphate dosing was observed. Addition of NaOH removed a maximum of 7 % of $\rm Mg^{2+}$ at pH 9.

3.2. Vivianite precipitation in reverse osmosis concentrate

The addition of phosphate resulted in removal of Fe²⁺, Mn²⁺ and Ca²⁺ in anaerobic concentrate (Fig. 2). No significant Mg²⁺ removal was obtained by phosphate addition (Fig. 2d), aligning with our observations for groundwater (Fig. 1). At elevated pH, higher removal efficiencies were found for all divalent cations. For Fe²⁺, a maximum removal of

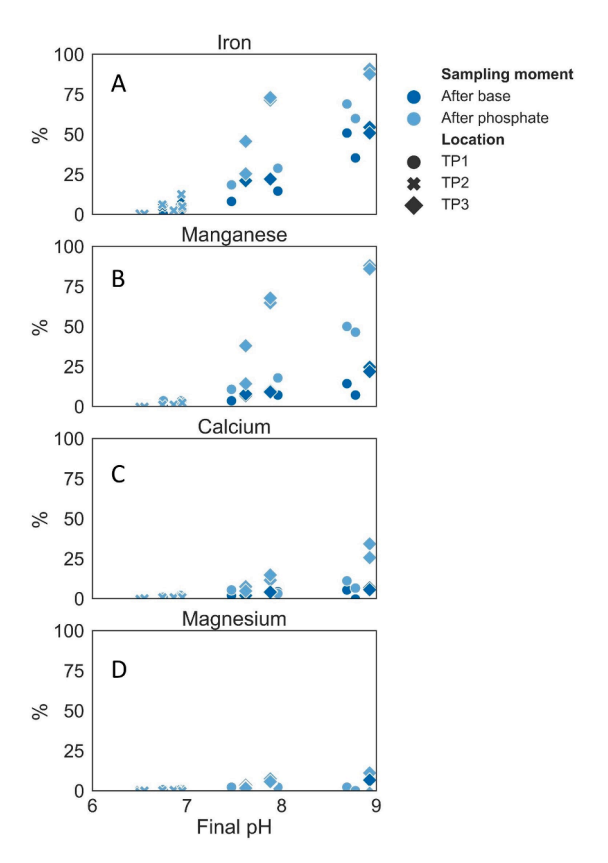


Fig. 1. Removal efficiencies of A) Fe^{2+} , B) Mn^{2+} , C) Ca^{2+} & D) Mg^{2+} in anaerobic groundwater at TP1 (circles) TP2 (crosses) TP3 (diamonds) after dosing different amounts of the base NaOH (dark blue) and after dosing phosphate as $Na_3(PO_4)_2$ with Fe/PO_4 ratio of 1 (light blue).

52 % was found, corresponding to a removal of 19 mg Fe/L. Addition of the base prior to phosphate dosing already removed 15 % of Fe. For $\rm Mn^{2+}$, a maximum removal of 49 % was found, corresponding to 0.65 mg Mn/L. The maximum $\rm Ca^{2+}$ removal was 13 %, corresponding to 58 mg Ca/L.

The highest removal efficiencies were found at TP1, since the pH of the concentrate was raised further compared to TP2. The initial concentrations of the divalent ions in the concentrates varied, as presented in Table 1. Around pH 7.3, the removal percentages of Fe²⁺, Mn²⁺ and Ca²⁺ were higher at TP2 (24 mg Fe/L, 0.95 mg Mn/L, 48 mg Ca/L) compared to TP1 (12 mg Fe/L, 0.32 mg Mn/L, 28 mg Ca/L).

3.3. Manganese removal during vivianite precipitation

In the on-site experiments using anaerobic groundwater and RO concentrate, co-removal of $\rm Mn^{2+}$ was observed during vivianite precipitation. The influence of $\rm Mn^{2+}$ on vivianite precipitation was therefore further studied under controlled lab conditions. Fig. 3 shows the removal of $\rm Mn^{2+}$ during vivianite precipitation at different concentrations, as presented in Table 2. In both Mn I and Mn II, 91 % of $\rm Mn^{2+}$ and 90 % of Fe²⁺ were removed. At Mn III, the highest $\rm Mn^{2+}$ concentration tested, 74 % $\rm Mn^{2+}$ removal was obtained and 68 % of Fe²⁺ (120 mg Fe/L) was removed. Under all investigated manganese concentrations, partial but significant $\rm Ca^{2+}$ co-removal was found (4.0–5.5 mg/L), while no significant $\rm Mg^{2+}$ removal was observed.

3.4. Calcium removal during vivianite precipitation

The removal of Ca^{2+} during vivianite precipitation was tested under seven different conditions (Fig. 4). The average removal percentage was 10 % and the maximum absolute removal was found at Ca VI (61.5 mg

R. Goedhart et al. Water Research 285 (2025) 124101

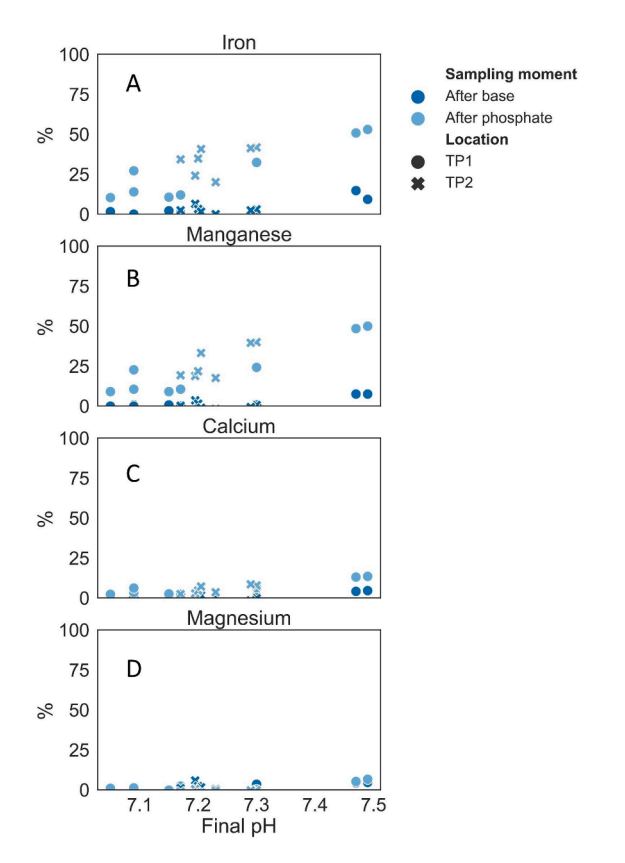


Fig. 2. Removal efficiencies of A) Fe^{2+} , B) Mn^{2+} , C) Ca^{2+} & D) Mg^{2+} in anaerobic groundwater concentrate after dosing different amounts of the base NaOH (dark blue) and after dosing phosphate as $Na_3(PO4)_2$ with Fe/PO_4 ratio of 1 (light blue) at TP1 (circles) & TP2 (crosses).

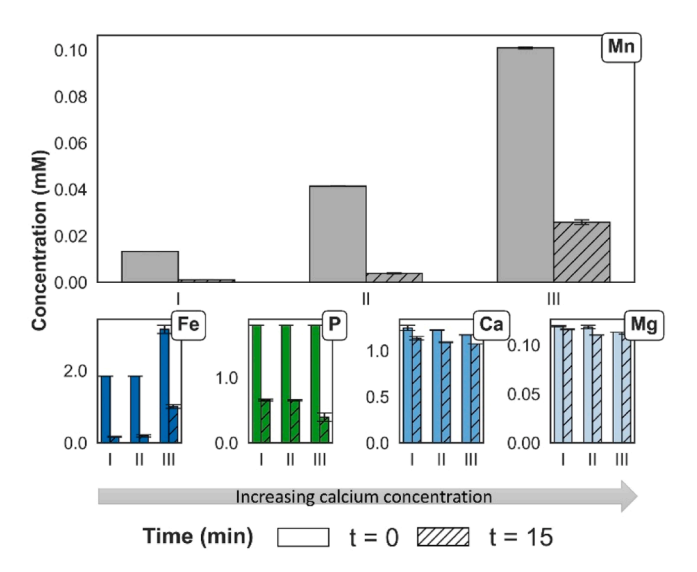


Fig. 3. Concentrations of Mn²⁺, Fe²⁺, P, Ca²⁺ & Mg²⁺ before and 15 min after the addition of 0.1 M sodium phosphate to groundwater spiked with 0.179 mM Fe²⁺ and of I) 0.009 II) 0.04 or III) 0.09 mM of Mn²⁺. Error bars are SD of n = 2.

Ca/L). Note that, although the removal efficiencies were lower compared to $\mathrm{Mn^{2+}}$, the absolute concentrations removed were much higher, because the concentration of $\mathrm{Ca^{2+}}$ present in concentrate streams is around 250 times higher compared to $\mathrm{Mn^{2+}}$. The removal of $\mathrm{Fe^{2+}}$ decreased at increasing $\mathrm{Ca^{2+}}$ concentrations, while the phosphate removal was unaffected. The dilution needed to measure $\mathrm{Ca^{2+}}$ lowered the concentration of $\mathrm{Mg^{2+}}$ and $\mathrm{Mn^{2+}}$ below detection limit of the ICP-MS

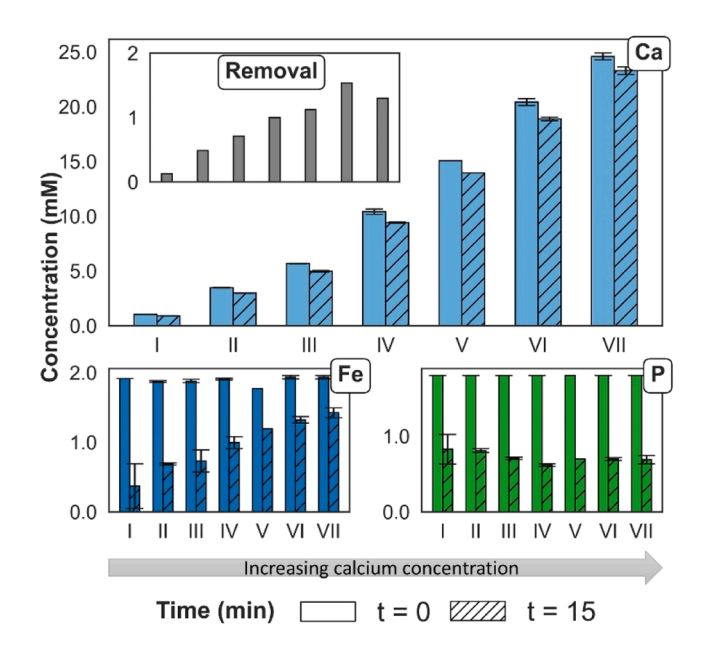


Fig. 4. Concentrations of Ca^{2+} , Fe^{2+} and P before and 15 min after the addition of 0.1 M sodium phosphate to groundwater spiked with 0.179 mM Fe^{2+} and Ca^{2+} ranging between 0 (I) and 25 (VII) mM. Mg^{2+} and Mn^{2+} concentrations are below detection limit and therefore not shown. Error bars are SD of n=2.

and are thus not included in these results.

3.5. Magnesium removal during vivianite precipitation

Fig. 5 shows the removal of magnesium during vivianite precipitation at different magnesium concentrations. The experiments Mg I and Mg II, containing 10 and 40 mg Mg/L, showed no significant removal of Mg $^{2+}$, while 88 % and 77 % of Fe $^{2+}$ were removed, respectively. A significant decrease of 7.2 % was only found for the highest tested Mg $^{2+}$ concentration of 80 mg Mg/L at which 84 % of Fe $^{2+}$ was removed. Partial Ca $^{2+}$ co-removal was found (4.0–5.5 mg/L), which aligned with the removal found in the Mn $^{2+}$ experiments.

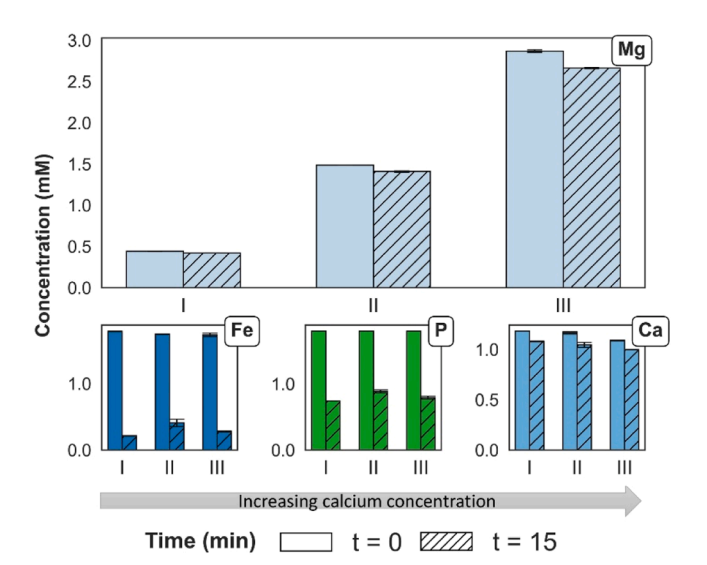


Fig. 5. Concentration of Mg^{2+} , Fe^{2+} , P and Ca^{2+} before and 15 min after the addition of 0.1 M sodium phosphate to groundwater spiked with 0.179 mM Fe^{2+} and of I) 0.4 II) 1.6 or III) 3.3 mM of Mg^{2+} . Mn^{2+} concentrations are below detection limit and therefore not shown. Error bars are SD of n=2.

R. Goedhart et al. Water Research 285 (2025) 124101

3.6. Co-removal of Mn^{2+} and Mg^{2+} does not affect mineral structure of vivianite

Fig. 6 shows SEM-EDS images of vivianite formed in the experiments Mn III and Mg III. The typical sheet-shaped flowers of vivianite were observed in both environments. The addition of $\mathrm{Mn^{2+}}$ or $\mathrm{Mg^{2+}}$ did not lead to observable morphological changes. The XRD pattern of the precipitates formed in the presence of $\mathrm{Mn^{2+}}$ or $\mathrm{Mg^{2+}}$ all showed vivianite (Figure S3). However, the presence of magnesium phosphate hydrate ($\mathrm{Mg_3(PO_4)_2(H_2O)_8}$) is difficult to exclude, because the main peaks appear at similar 2theta values. The XRD pattern of Mg III shows that amorphous structures were present in the sample alongside vivianite. An element map was made for the precipitated solids at Mn III and Mg I, which shows that the elements Fe, P and O were evenly distributed (Figure S4). $\mathrm{Mg^{2+}}$ and $\mathrm{Mn^{2+}}$ were not detected, because of the low concentration precipitated compared to $\mathrm{Fe^{2+}}$ and P.

3.7. Calcium outcompetes iron for phosphate

The XRD pattern of the precipitates formed in experiments Ca II, Ca III, Ca IV and Ca VII all show the presence of vivianite (Fig. 7). At higher ${\rm Ca^{2+}}$ concentrations, the peaks were broadened, meaning that amorphous structures were present alongside the crystalline vivianite. Calcium-phosphate precipitates have likely formed; Fig. 4 shows that phosphate removal was independent of the ${\rm Ca^{2+}}$ concentration present, while ${\rm Fe^{2+}}$ removal decreased at higher ${\rm Ca^{2+}}$ concentrations. Calcium outcompeted ${\rm Fe^{2+}}$ for precipitation with phosphate. The presence of ${\rm Fe^{2+}}$, P, O and ${\rm Ca^{2+}}$ were evenly distributed over the precipitated solid (Fig S3); no separate clusters of Ca-P and Fe-P were found.

4. Discussion

${\it 4.1.}\ \ Incorporation\ of\ manganese\ and\ magnesium\ in\ the\ vivianite\ structure$

Iron recovery via vivianite precipitation was not found to be limited by the co-occurrence of divalent cations Mg^{2+} or Mn^{2+} in concentrations relevant to groundwater concentrates. Vivianite precipitation additionally removed Mn²⁺ up to 91 %, while similar Fe²⁺ removal efficiencies were maintained. Removal of Mg²⁺ at 10 or 40 mg/L was not significant, but a significant 7 % was removed at an initial Mg concentration of 80 mg/L. Again, this Mg removal did not hinder the removal of $\mathrm{Fe^{2+}}$. Note that this 7 % $\mathrm{Mg^{2+}}$ removal corresponds to approximately 5.5 mg/L, which is higher than the total concentration of Mn²⁺ added in the Mn-experiments. In groundwater and many other aqueous environments, Mg^{2+} concentrations are generally higher than Mn^{2+} . Despite the higher concentrations of Mg^{2+} present, Mn^{2+} substitution in vivianite was more successful in groundwater and concentrate. This aligns with findings in literature, where favorable Mn²⁺ substitution even at large Mg/Mn ratio is also reported (Egger et al., 2015; Kubeneck et al., 2023, 2021).

Substitution of ${\rm Mn}^{2+}$ in the vivianite crystal can result in pits and rosettes of a smaller size, and substitution by ${\rm Mg}^{2+}$ can lead to more

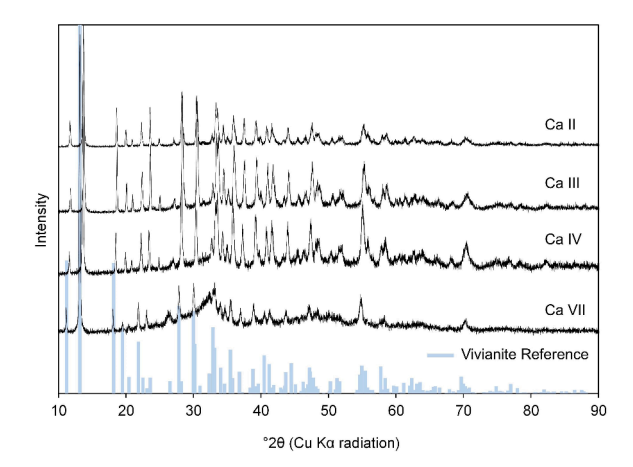


Fig. 7. XRD pattern of the precipitates formed in experiments Ca II, Ca III, Ca IV and Ca VII and a reference pattern of vivianite (blue).

platy globular structures and thicker crystals (Kubeneck et al., 2023). In our study, no structural changes of vivianite were identified in the presence of $\mathrm{Mn^{2+}}$ or $\mathrm{Mg^{2+}}$ (Fig. 6). The highest $\mathrm{Mn/Fe}$ ratio tested was 0.05, which is a 150 times lower ratio compared to the study of Joëlle Kubeneck et al. (2023). The concentrations relevant to groundwater or RO concentrate are probably too low to cause detectable morphological effects by the substitution of $\mathrm{Mn^{2+}}$ or $\mathrm{Mg^{2+}}$.

Recovery of vivianite from the water stream can be achieved by magnetic separation (Prot et al., 2019). For application purposes, it should be taken into account that impurities like manganese and magnesium can decrease the extraction efficiency of iron and phosphate from the recovered vivianite (Bec et al., 2025).

4.2. Calcium hinders iron recovery via vivianite precipitation

While Mn²⁺ and Mg²⁺ did not disturb Fe²⁺ removal during vivianite precipitation, the presence of Ca²⁺ did lower the Fe²⁺ removal efficiency. However, the concentrations of phosphate precipitated remained unaffected by the addition of Ca²⁺. This indicates that Fe²⁺ and Ca²⁺ compete for phosphate, and Ca²⁺ competes with Fe²⁺ in the vivianite crystallization process, thereby decreasing the purity of vivianite (Cao et al., 2023). At increasing Ca2+ concentrations, the Fe/P ratio removed became significantly lower, as previously reported by Chen et al. (2022). In our study, at 1000 mg/L Ca^{2+} , the Fe/PO₄ ratio dropped from the theoretical molar ratio of 1.5 to 0.5. This ratio is much lower compared to the Fe/PO₄ ratio of 1.24 (at 1280 mg/L Ca²⁺) as found by Chen et al. (2022). Two mechanisms can be responsible for the inhibition of Fe^{2+} removal when Ca^{2+} is present: i) Ca^{2+} replaces Fe^{2+} in the vivianite crystal and/or ii) Ca²⁺ precipitates with phosphate to form another mineral, most likely hydroxyapatite Ca5(PO4)3 (HAP) or tricalcium phosphate Ca₃(PO₄)₂. Fig. 8 shows the fractions of Fe, Ca and P removed in the experiments at different Ca concentrations and the theoretical ratios of HAP, vivianite and tricalcium phosphate. The ratio

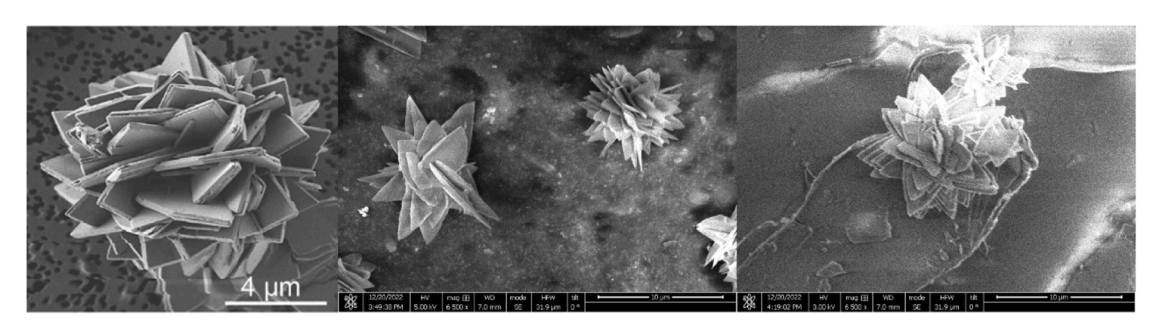


Fig. 6. Scanning electron microscopy images of A) pure vivianite obtained from Joëlle Kubeneck et al. (2023), B) experiment Mn III and C) experiment Mg III.

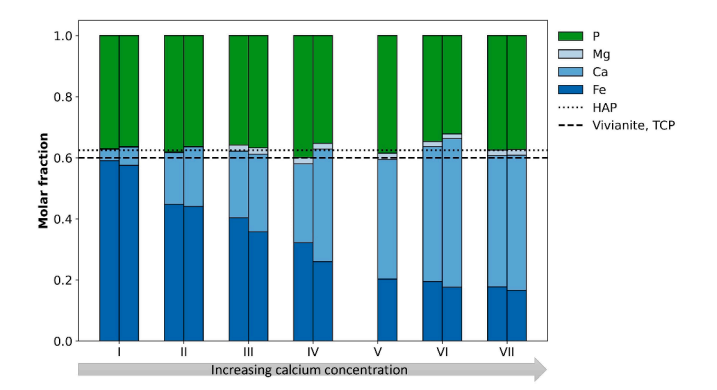


Fig. 8. Molar fraction of removed Fe, Ca, Mg and P in experiments Ca I – Ca VII. The theoretical fractions of phosphate in Vivianite, Tricalcium phosphate (TCP) and Hydroxyapatite (HAP) are also given.

 $PO_4/(Fe+PO_4)$ in vivianite and tricalcium phosphate is 0.4 and the ratio $PO_4/(Ca+PO_4)$ in HAP is 0.375. These nearly identical ratios make it difficult to distinguish which precipitate formed. Fig. 8 shows that at different Ca^{2+} concentrations the ratios were indeed always around these values.

XRD analysis showed the characteristic peaks of vivianite at all the different Ca^{2+} concentrations measured (Fig. 7), while Cao et al. (2023) lost the vivianite signal at 100 mg Ca/L and similar Fe^{2+} concentration. At higher Ca^{2+} concentrations, we did see a decrease of intensity of the main peaks and a broadened pattern, which indicates the presence of amorphous structures. Cao et al. (2023) showed that this decrease in crystallinity is caused by the formation of $\text{Ca}_3(\text{PO}_4)_2$ covering the surface of the vivianite crystals, which eventually inhibits vivianite crystallization. They report that inhibition starts from 50 mg/L, while we detected crystalline vivianite even at a concentration of 1000 mg/L of Ca^{2+} . Figure S4 shows that Ca^{2+} and Fe^{2+} are evenly distributed, suggesting that indeed Ca-PO_4 particles cover the vivianite surface.

4.3. Practical relevance

The concept of vivianite precipitation for iron recovery from concentrate shows promising results in batch experiments. To scale up this technology, the method should be further tested in a continuous flow system. In previous work, the halftime of iron removal via vivianite precipitation was found to be 4 min ($k=2.3~{\rm M}^{-1}~{\rm s}^{-1}$) at an initial concentration of 100 mg Fe²⁺/L (Goedhart et al., 2022). In the current study, efficient iron removal occurred in batch experiments of 15 min. These fast kinetics suggest that upscaling to a continuous flow reactor with a residence time of around 15 min would be feasible. The use of seeding crystals could further enhance the precipitation rate (Liu et al., 2018).

To minimize competition between Ca²⁺ and Fe²⁺ for phosphate, a pre-treatment step to remove calcium, such as an ion exchange resin, is recommended. An appealing alternative option is the implementation of a pellet reactor to precipitate CaCO3; a well-established softening technique in drinking water treatment (Graveland et al., 1983). More recently, this method has also been tested for RO concentrate treatment, achieving efficient Ca²⁺ removal (70–95 %) and partial removal of Mg²⁺ (5-25 %) (Tran et al., 2012). Another advantage of implementing a pellet reactor is the base dosing, which increases the pH of the stream and thereby promoting vivianite formation. The pre-treatment step removing Ca^{2+} will also result in better extraction efficiencies to eventually recover the iron and phosphate from the vivianite (Bec et al., 2025). Fig. 9 presents a conceptual treatment scheme that incorporates both a pellet reactor and vivianite precipitation. The most suitable reactor design for vivianite precipitation should be explored in a next study.

In the presented study, phosphate was slightly overdosed (P:Fe ratio

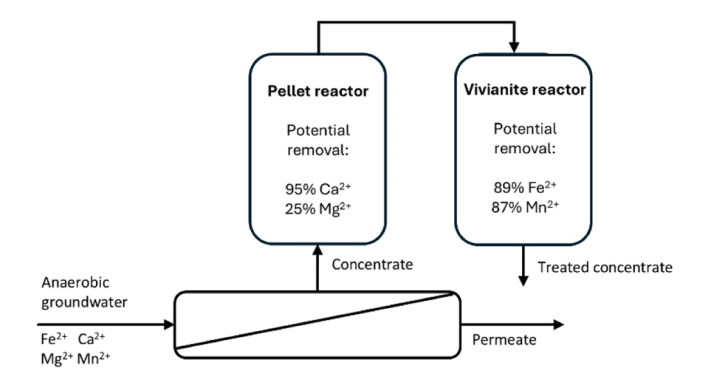


Fig. 9. Schematic overview of a possible treatment scheme for RO concentrate treatment. Step 1: A pellet reactor recovering calcium and increasing the pH. Step 2: A reactor for vivianite precipitation recovering iron.

of 1:1 instead of theoretical ratio of 1:1.5) to avoid limitation of the reactant. However, for full-scale application, overdosing of phosphate should be avoided. Residual phosphate in the treated water would be undesirable, and unnecessary chemical use also increases the costs. Another consideration is that incomplete phosphate removal was observed in some experiments, even when ${\rm Fe}^{2+}$ and ${\rm Ca}^{2+}$ were still available. This might indicate that the SI dropped below the threshold required for vivianite formation (Goedhart et al., 2022). Optimizing the phosphate dose, based on the water's SI and pH, will be essential before scaling up. Antiscalants present in the concentrate stream can also influence the optimal phosphate dose; smart selection of P-containing antiscalants might be beneficial for vivianite precipitation. The effect of different antiscalants on vivianite precipitation should be studied before scaling up.

Implementing a treatment scheme as proposed in Fig. 9 can change the way RO concentrate is perceived in the industry. Rather than viewing concentrate as a byproduct, it can be recognized as a valuable stream. It supports the increasing trend towards resource recovery in water treatment and contributes to the environmental and economic sustainability of the sector.

5. Conclusion

This study shows evidence that vivianite can effectively precipitate across a wide range of groundwater matrices. Iron recovery via vivianite precipitation is a novel solution to manage streams such as membrane concentrate that are currently difficult to treat due to high levels of iron and calcium. Our results indicate that divalent ions manganese and calcium are co-removed during the process, while magnesium removal was limited to only 7 % removal at high concentrations (80 mg Mg^{2+}/L). The presence of manganese and magnesium did not hinder the iron recovery or alter the crystalline structure of vivianite formed. The coremoval of calcium during vivianite precipitation occurred at the expense of iron removal, with the formation of amorphous calcium phosphate precipitates. Further investigation is required to determine if the divalent ions are incorporated into the vivianite structure itself, or if other precipitates form. This study underscores the potential of vivianite precipitation as a method for treating anaerobic concentrate streams and highlights the need for further research to optimize this novel treatment process.

CRediT authorship contribution statement

Roos Goedhart: Writing – review & editing, Writing – original draft, Visualization, Validation, Supervision, Project administration, Methodology, Investigation, Funding acquisition, Formal analysis, Data curation, Conceptualization. Nienke Koudijs: Writing – review & editing, Visualization, Validation, Methodology, Investigation, Formal analysis,

Data curation, Conceptualization. **Mark C.M. van Loosdrecht:** Writing – review & editing, Validation, Methodology, Conceptualization. **Doris van Halem:** Writing – review & editing, Validation, Supervision, Methodology, Formal analysis.

Declaration of competing interest

The authors declare that they have no known competing financial interests or personal relationships that could have appeared to influences the work reported in this paper.

Acknowledgements

This research is funded by NWO Dutch Science Council (grant 19541). The authors would like to thank Frank Schoonenberg, Klaas Gorter (Vitens) and Tjark Holst (TU Delft) for support in fieldwork, Jane Erkemeij (TU Delft) for ICP-MS analysis, Arjan Thijssen (TU Delft) for SEM-EDS measurements, Xiaohui Liu and Ruud Hendrikx (TU Delft) for XRD analyses and Ben Abbas (TU Delft) for support with the anaerobic chamber.

Supplementary materials

Supplementary material associated with this article can be found, in the online version, at doi:10.1016/j.watres.2025.124101.

Data availability

Data will be made available on request.

References

- AquaMinerals, 2020. Annual Report 2019.
- Bec, S., Prot, T., Dugulan, I.A., Korving, L., Mänttäri, M., 2025. The challenges and limitations of vivianite quantification with 2,2'-bipyridine extraction. Sci. Total. Environ. 972. https://doi.org/10.1016/j.scitotenv.2025.179112.
- Cao, J., Zhao, W., Wang, S., Xu, R., Hao, L., Sun, W., 2023. Effects of calcium on phosphorus recovery from wastewater by vivianite crystallization: interaction and mechanism analysis. J. Environ. Chem. Eng. 11, 2213–3437. https://doi.org/ 10.1016/j.jece.2023.110506.
- Chen, X., Zheng, M., Cheng, X., Wang, C., Xu, K., 2022. Resources, conservation & recycling impact of impurities on vivianite crystallization for phosphate recovery from process water of hydrothermal carbonization of kitchen waste. Resour. Conserv. Recycl. 185, 106438. https://doi.org/10.1016/j.resconrec.2022.106438.
- Egger, M., Jilbert, T., Behrends, T., Rivard, C., Slomp, C.P., 2015. Vivianite is a major sink for phosphorus in methanogenic coastal surface sediments. Geochim. Cosmochim. Acta 169, 217–235. https://doi.org/10.1016/J.GCA.2015.09.012.
- Goedhart, R., Müller, S., van Loosdrecht, M.C.M., van Halem, D., 2022. Vivianite precipitation for iron recovery from anaerobic groundwater. Water. Res. 217, 118345. https://doi.org/10.1016/J.WATRES.2022.118345.
- Graveland, A., Dijk, J.C.van, de Moel, P.J., Oomen, J.H.C.M., 1983. Developments in water softening by means of pellet reactors. J. Am. Water. Works. Assoc. 75, 619–625. https://doi.org/10.1002/J.1551-8833.1983.TB05247.X.

- Haukelidsaeter, S., Boersma, A.S., Piso, L., Lenstra, W.K., van Helmond, N.A.G.M., Schoonenberg, F., van der Pol, E., Hurtarte, L.C.C., van der Wielen, P.W.J.J., Behrends, T., van Kessel, M.A.H.J., Lücker, S., Slomp, C.P., 2024. Efficient chemical and microbial removal of iron and manganese in a rapid sand filter and impact of regular backwash. Appl. Geochemistry 162, 105904. https://doi.org/10.1016/j. apgeochem.2024.105904.
- Kloprogge, J.T., Visser, D., Martens, W.N., Duong, L.V., Frost, R.L., 2003. Identification by RAMAN microscopy of magnesian vivianite formed from Fe2+, Mg, Mn2+ and PO43- in a Roman camp near fort Vechten, Utrecht, The Netherlands. Geol. en Mijnbouw/Netherlands J. Geosci. 82, 209–214. https://doi.org/10.1017/ s0016774600020758.
- Kubeneck, L.J., Lenstra, W.K., Malkin, S.Y., Conley, D.J., Slomp, C.P., 2021. Phosphorus burial in vivianite-type minerals in methane-rich coastal sediments. Mar. Chem. 231, 103948. https://doi.org/10.1016/j.marchem.2021.103948.
- Kubeneck, L.J., ThomasArrigo, L.K., Rothwell, K.A., Kaegi, R., Kretzschmar, R., 2023. Competitive incorporation of Mn and Mg in vivianite at varying salinity and effects on crystal structure and morphology. Geochim. Cosmochim. Acta 346, 231–244. https://doi.org/10.1016/j.gca.2023.01.029.
- Liu, J., Cheng, X., Qi, X., Li, N., Tian, J., Qiu, B., Xu, K., Qu, D., 2018. Recovery of phosphate from aqueous solutions via vivianite crystallization: thermodynamics and influence of pH. Chem. Eng. J. 349, 37–46. https://doi.org/10.1016/j. cei.2018.05.064.
- Morris, M.C., McMurdie, H.F., Evans, E.H., Paretzkin, B., de Groot, J.H., Hubbard, C.R., Carmel, S.J., 1979. Standard X-ray diffraction powder patterns: section 16 - data for 86 substances.
- Müller, S., Corbera-Rubio, F., Schoonenberg Kegel, F., Laureni, M., van Loosdrecht, M.C. M., van Halem, D., 2024. Shifting to biology promotes highly efficient iron removal in groundwater filters. Water. Res. 262, 122135. https://doi.org/10.1016/j. watres.2024.122135.
- Nederlof, M.M., van Paassen, J.A.M., Jong, R., 2005. Nanofiltration concentrate disposal: experiences in he Netherlands. Desalination. 178, 303–312. https://doi.org/ 10.1016/j.desal.2004.11.041.
- Pérez-González, A., Urtiaga, A.M., Ibáñez, R., Ortiz, I., 2012. State of the art and review on the treatment technologies of water reverse osmosis concentrates. Water. Res. 46, 267–283. https://doi.org/10.1016/j.watres.2011.10.046.
- Prot, T., Nguyen, V.H., Wilfert, P., Dugulan, A.I., Goubitz, K., De Ridder, D.J., Korving, L., Rem, P., Bouderbala, A., Witkamp, G.J., van Loosdrecht, M.C.M., 2019. Magnetic separation and characterization of vivianite from digested sewage sludge. Sep. Purif. Technol. 224, 564–579. https://doi.org/10.1016/j.seppur.2019.05.057.
- Rothe, M., Kleeberg, A., Hupfer, M., 2016. The occurrence, identification and environmental relevance of vivianite in waterlogged soils and aquatic sediments. Earth-Science Rev 158, 51–64. https://doi.org/10.1016/J.EARSCIREV.2016.04.008.
- Schipper, P.N.M., Vissers, M.J.M., van der Linden, A.M.A., 2008. Pesticides in groundwater and drinking water wells: overview of the situation in The Netherlands. Water. Sci. Technol. 57, 1277–1286. https://doi.org/10.2166/wst.2008.255.
- Tran, A.T.K., Zhang, Y., Jullok, N., Meesschaert, B., Pinoy, L., Van der Bruggen, B., 2012. RO concentrate treatment by a hybrid system consisting of a pellet reactor and electrodialysis. Chem. Eng. Sci. 79, 228–238. https://doi.org/10.1016/j.ces.2012.06.001.
- Turner, T., Wheeler, R., Stone, A., Oliver, I., 2019. Potential alternative reuse pathways for water treatment residuals: remaining barriers and questions-a review. Water. Air. Soil. Pollut. 230. https://doi.org/10.1007/s11270-019-4272-0.
- Van Beek, C.G.E.M., Hiemstra, T., Hofs, B., Nederlof, M.M., Van Paassen, J.A.M., Reijnen, G.K., 2012. Homogeneous, heterogeneous and biological oxidation of iron(II) in rapid sand filtration. https://doi.org/10.2166/aqua.2012.033.
- World Health Organization, 2017. Guidelines For Drinking-Water Quality, 4th edition. WHO Library Cataloguing-in-Publication Data, Geneva. incorporating the 1st addendum, Licence: CC BY-NC-SA 3.0 IGO.
- Zamrsky, D., Oude Essink, G.H.P., Bierkens, M.F.P., 2024. Global impact of sea level rise on coastal fresh groundwater resources. Earth's Futur 12. https://doi.org/10.1029/ 2023FF003581.